Journal of Advanced Research 61 (2024) 165–178

Contents lists available at ScienceDirect

Journal of Advanced Research

journal homepage: www.elsevier.com/locate/jare

Intracellular *Fusobacterium nucleatum* infection increases METTL3-mediated m6A methylation to promote the metastasis of esophageal squamous cell carcinoma

Songhe Guo [a,1], Fangfang Chen [b,1], Linfang Li [a,1], Shuheng Dou [b], Qifan Li [b], Yuying Huang [b], Zijun Li [c,*], Wanli Liu [a,*], Ge Zhang [b,*]

[a] State Key Laboratory of Oncology in South China, Collaborative Innovation Center for Cancer Medicine, Sun Yat-sen University Cancer Center, Guangzhou, China
[b] Department of Microbial and Biochemical Pharmacy, School of Pharmaceutical Sciences, Sun Yat-sen University, Guangzhou, China
[c] Department of General Practice, Concord Medical Center, Institute of Geriatrics, Guangdong Provincial People's Hospital (Guangdong Academy of Medical Sciences), Southern Medical University, Guangzhou, China

HIGHLIGHTS

- Fn was positively correlated with METTL3 expression in the ESCC tissues.
- Fn-infection induced the upregulated-expression of METTL3 in ESCC.
- Fn mediated METTL3/Myc axis to promote ESCC cells proliferation and migration *in vitro*.
- Fn accelerates ESCC tumorigenesis and metastasis via METTL3-mediated c-Myc mRNA m6A modification *in vivo*.

GRAPHICAL ABSTRACT

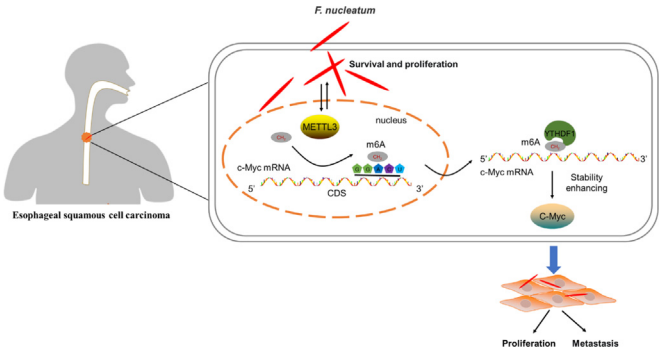

ARTICLE INFO

Article history:
Received 20 June 2023
Revised 17 August 2023
Accepted 21 August 2023
Available online 22 August 2023

Keywords:
Fusobacterium nucleatum
METTL3
m6A methylation
c-Myc
Esophageal squamous cell carcinoma

ABSTRACT

Introduction: The tumor-associated microbiota plays a vital role in cancer development. Accumulating evidence shows that *Fusobacterium nucleatum* (Fn) participates in the progression of multiple tumor types. However, the underlying mechanisms remain unclear.
Objectives: This study examined the expression of methyltransferase-like protein 3 (METTL3) during Fn infection and elucidated the function and pathway of Fn-induced m6A methylation in esophageal squamous cell carcinoma (ESCC).
Methods: The abundance of Fn in patient tissues was determined by qPCR. Western blot, qRT-PCR, and immunohistochemistry were performed to measure METTL3 expression in cells and tissues. METTL3 function was evaluated *in vitro* by colony formation and cell migration assays. MeRIP-qPCR was performed to determine the relationship between METTL3 and c-Myc. In addition, the half-lives of genes that are downstream of METTL3 were determined with RNA stability assays.
Results: Fn was enriched in hepatocellular carcinoma (HCC), breast cancer (BRCA), ESCC, and colorectal cancer (CRC) tumor tissues. METTL3 expression was positively associated with Fn abundance in ESCC

Abbreviations: Fn, *Fusobacterium nucleatum*; ESCC, esophageal squamous cell carcinoma; m6A, N6-methyladenosine; METTL3, methyltransferase-like 3; qPCR, quantitative real-time PCR; qRT-PCR, quantitative reverse transcription PCR; IF, immunofluorescence; IHC, immunohistochemistry; MOI, multiplicity of infection; LSCM, laser scanning confocal microscope; GEPIA, Gene Expression Profiling Interactive Analysis; YTHDF1, YTH N6-Methyladenosine RNA Binding Protein 1; RIP-qPCR, RNA immunoprecipitation followed by qPCR; OE, overexpression.

* Corresponding authors.
E-mail addresses: zijunli2005@aliyun.com (Z. Li), liuwl@sysucc.org.cn (W. Liu), zhangge@mail.sysu.edu.cn (G. Zhang).

[1] ***Authorship:*** Songhe Guo, Fangfang Chen, and Linfang Li have contributed equally to this work.

https://doi.org/10.1016/j.jare.2023.08.014

tissues. Fn could survive and proliferation as well as increase METTL3 expression in ESCC, HCC, CRC, and BRCA cells. Moreover, METTL3 overexpression promoted ESCC cells proliferation, migration *in vivo* and *in vitro*. Mechanistically, Intracellular Fn infection increases METTL3 transcription. METTL3 promoted c-Myc mRNA methylation in the 3′-untranslated Region (3′-UTR) and enhanced its mRNA stability in a YTH N6-Methyladenosine RNA binding protein 1(YTHDF1)-dependent manner, which contributes to Fn induced ESCC proliferation and metastasis.

Conclusions: This study indicates that intracellular Fn infection promotes ESCC development and metastasis, and eradicating Fn infection may be a promising strategy for treating ESCC.

Introduction

The posttranscriptional RNA modification known as N6-methyladenosine (m6A) is highly prevalent in mammalian mRNA and has been associated with various physiological and pathological mechanisms [1,2]. The addition of m6A modification can be achieved by m6A methyltransferases, and its removal is mediated by demethylases. Additionally, m6A-binding proteins are responsible for recognizing this alteration [3]. Dysregulation of m6A modification because of the aberrant expression of regulatory proteins is related to the pathogenesis of various disorders, particularly cancer [4,5].

Methyltransferase-like protein 3 (METTL3) is a crucial component of the m6A methyltransferase complex with significant importance. A body of research indicates that METTL3 plays a role in the interaction with tumor cells and the progression of various malignant conditions [4,6]. Importantly, abnormal expression of METTL3 is frequently observed in various types of carcinoma, including colorectal cancer and esophageal cancer [7,8], and increasing evidence confirms that elevated METTL3 levels are related to a worse prognosis in patients with these tumors [9,10]. Thus, although controversial, most current studies suggest that METTL3 performs an oncogenic function in the progression of cancer.

Recently, intratumoral bacteria,which are newly recognized components of tumors, have been observed in various types of cancers, but their biological roles remain undetermined [11,12]. Fusobacterium *nucleatum* (Fn) is an obligate anaerobic proinflammatory bacterium which has been identified as a facultative intracellular bacterium in our previous study [13]. A growing body of research has demonstrated that Fn functions as an oncogenic bacterium, and the overabundance of Fn in the intestinal tract is implicated the progression of several cancers, including esophageal, gastric, colon, breast, and pancreatic cancers [14–18]. Furthermore, several new investigations determined that Fn is an important intratumoral bacterium in both colorectal cancer (CRC) and oral squamous cell carcinoma (OSCC) [11,19].

Esophageal squamous cell carcinoma (ESCC) is the predominated histological type of esophageal cancer and highly prevalent in Asia [20]. Recently, several studies verified that m6A levels were elevated in ESCC cells and tissues, and upregulated METTL3 expression was also observed in ESCC tissues and was related to worse prognosis [8,21–23]. Additionally, multiple recent studies confirmed that Fn is highly abundant in ESCC tissues and promotes cancer progression [15,24], and Fn infection predicts a high risk of metastasis in ESCC [25]. However, it is unknown whether and how intratumoral Fn regulates m6A methylation in ESCC.

Chronic persistent infection is the most crucial epigenetic factor contributing to tumor progression. Currently, the extent to which intratumoral bacteria may impact m6A modification in tumor cells remains largely unknown. Recently, a study showed that Fn decreases m6A modification levels by downregulating METTL3 in CRC cells and xenograft tumor tissues [26]. However, this result is inconsistent with the observation that increasing METTL3 expression may be accompanied by Fn enrichment in CRC tissues [27].

In the present study, we focused on the role of METTL3-mediated m6A methylation during Fn infection, and described the role and mechanism of METTL3 secreted from Fn-infected cells on ESCC progression and development. These findings might promote a novel insight for the ESCC treatment.

Materials and methods

Patients and specimen collection

Twenty-two ESCC tumor tissues and paired adjacent normal tissues were collected at the Third Affiliated Hospital of Sun Yat-Sen University Yuedong Hospital. The study sample included 22 individuals, 12 males with a mean age of 61 years and 10 females with a mean age of 59 years. All ESCC patients were newly diagnosed and confirmed by histopathological examination under the 7th edition of the TNM-UICC/AJCC classification. All enrolled patients were first diagnosed and didn't receive antibiotic therapy within one month. Patients with coexisting autoimmune, chronic, and acute inflammatory diseases were excluded from the study.

Bacterial strains and culture conditions

Fn ATCC 25586 and ESCC tissue-derived Fn strains (ESCC-Fn) were cultured anaerobically for two to three days at 37 °C in brain heart infusion broth (BHI, Oxoid, UK). *E. coli* (DH5α; Tiangen, China) was cultivated aerobically on an LB agar plate for 24 h at 37 °C. Heat-killed Fn (K-Fn) was prepared by heating the bacteria at 100 °C for 0.5 h. In addition, the bacteria were suspended in RPMI-1640 medium (Gibco, USA) to a final concentration of 1×10^8 colony forming units (CFU) mL^{-1} for the infection experiment.

Cell culture

The Eca109, Kyse150, MDA-MB-231 (231), MCF7, HepG2, Huh7, HCT116, and SW480 cell lines were cultured in RPMI-1640 medium (Gibco) supplemented with 10% fetal bovine serum (FBS, Gibco). The cells were incubated at 37 °C in a humidified incubator with 5% CO_2.

RNA extraction and quantitative reverse transcription PCR (qRT-PCR)

Consistent with the manufacturer's instructions, total RNA was harvested from cells utilizing TRIzol Reagent (TaKaRa, China). First-strand cDNA was synthesized with a reverse transcription kit (AG, China). Quantitative real-time PCR was carried out with the Quan-

tiFast SYBR ® Green PCR Kit (AG, China) on a Bio-Rad CFX384 real-time PCR machine. The expression of the target cDNAs that were analyzed by real-time PCR was normalized to that of GAPDH. To determine the relative mRNA levels, we employed the $2^{-\Delta\Delta}$Ct method. **Table S1** provides a list of the PCR primers.

Establishment of stable cell lines

To achieve METTL3 overexpression, ESCC cells were stably transfected with the plasmid pcDNA3/Flag-METTL3 (Addgene #53739). The transfection procedure was conducted utilizing Lipofectamine 3000 (Invitrogen, USA) following the manufacturer's instructions. In summary, the cells were grown in six-well plates until they reached 90% confluence. ESCC cells were transfected with plasmid DNA (5.0 mg per well) and Lipofectamine 3000 to facilitate transfection. After 48 h, the cells were subjected to trypsinization and subsequently transferred to 10-cm culture dishes in medium supplemented with 300 mg/mL G418 (Gibco, USA). Clonal expansion was achieved through the isolation of single-cell clones.

Stable METTL3-knockdown cell lines were generated by a lentivirus-mediated small hairpin RNA (shRNA) knockdown system (GenePharma Co., Ltd., China). The shRNA target sequences are listed in **Table S1**. ESCC cells were transfected with target plasmids and viral packaging plasmids to generate lentiviral particles using the Trans-lentiviral Packaging Kit (Invitrogen, USA) according to the instructions of the kit. After 48 h of transfection, lentivirus particles were obtained and concentrated employing a Lenti-X concentrator in accordance with the manufacturer's instructions (Clontech). Lentivirus particles were utilized to transduce stable cell lines in serum-free medium with 8 μg/mL polybrene (Sigma, USA). Subsequently, the transduced cells were subjected to selection with 2 μg/mL puromycin for a minimum of ten days. METTL3 mRNA and protein expression in each cell clone was measured by screening via qRT-PCR and western blot analysis.

siRNA transfection

When ESCC cells reached 60% confluence in a six-well plate, they were transfected with either negative control small interfering RNA (siRNA) or c-Myc-specific siRNA (Shanghai Jikai Gene, China) at a final concentration of 30 nM for 24 h, following the manufacturer's instructions.

Immunofluorescence (IF) staining

Immunofluorescence staining was used to conduct bacterial invasion tests, as described in our previous study[13]. The experiment involved incubating the samples with a rabbit polyclonal anti-Fn antibody (created in-house, diluted to 1:5,000), anti-α-tubulin antibody (diluted to 1:200, Bioworld, USA), and anti-METTL3 antibody (diluted to 1:1,000, Abcam, USA) at 4 °C overnight. Subsequently, the secondary antibodies were added and coincubated at 4 °C overnight. Subsequently, the samples were incubated with fluorescent secondary antibodies, namely, anti-rabbit IgG (DyLight 594) and anti-mouse IgG (DyLight 488) (diluted to 1:100, Abcam, USA), for 40 min at ambient temperature. The nuclei were stained with DAPI (Beyotime, China) for 5 min. Image acquisition was performed using a laser scanning confocal microscope FV3000 (Olympus).

Intracellular survival assays

The evaluation of bacterial infection, including intracellular entry and growth, was conducted as described in our previous study[13]. The Kyse150 and Eca109 cell lines were infected with live Fn at a multiplicity of infection (MOI) of 10:1, followed by incubation at 37 °C in 5% CO_2 for 12 h. Next, the cells that were infected with Fn were subjected to three rounds of washing with PBS and then subjected to a 2 h incubation with gentamicin (100 μg/mL) to eliminate any bacteria that were present in the extracellular space. Finally, the cells were lysed in 0.5% Triton X-100 lysis buffer supplemented with protease and phosphatase inhibitors. The abundance of intracellular Fn was determined by cultivation on blood agar plates and counting of colony-forming units (CFU).

Western blot

The cells were lysed in RIPA buffer and subsequently exposed to boiling conditions for 10 min. The proteins were separated on a 10% SDS-PAGE gel, followed by transfer to PVDF membranes. The membranes were blocked by incubation with 5% skim milk powder for 2 h. Then, the membranes were incubated overnight with antibodies against METTL3 and c-Myc at a concentration of 1:2,000 (Abcam). After washing with PBST, the membranes were incubated with a horseradish peroxidase (HRP)-conjugated secondary antibody (1:5,000, CST, USA) for 2 h at room temperature. Then, GAPDH was used as an internal reference to determine the relative protein expression. Visualization of the protein bands was accomplished using a chemiluminescence detection system (Tianneng, China).

M6A-RIP and m6A sequencing assays (MeRIP-seq)

The Me-RIP procedure was carried out following previously described methods[28]. In summary, 50 μg RNA was isolated, and ribosomal RNA was removed with the use of a RiboMinus™ Eukaryote Kit v2 (A15020, Invitrogen). Subsequently, the RNA was fragmented into fragments of approximately 100 nucleotides with RNA fragmentation reagents (AM8740, Invitrogen). The residual samples were incubated and immunoprecipitated (at 4 °C for 2 h) with an anti-m6A antibody (CST, USA). Then, the methylated RNA was purified for further immunoprecipitation (MeRIP) sequencing by LC-Bio (Hangzhou, China).

Colony formation assay

The experiment involved seeding cells in 6-well plates at a density of 700 cells per well, followed by culture for a couple of weeks. Subsequently, the cells were fixed with 4% paraformaldehyde and stained with 1% crystal violet for colony quantification.

Scratch wound healing assay

After seeding cells in 60-mm dishes, a confluent monolayer was achieved. A "scratch" was established by scraping a straight line in the cell monolayer utilizing a p100 pipette tip. Forty-eight hours later, images of wound healing were captured to calculate the percentage of wound healing.

Transwell migration assay

Cell migration assays were conducted with 24-well Transwell inserts with a pore size of 8 μm (Merck Millipore, Germany). Serum-free RPMI-1640 medium and ESCC cells (1×10^5) were added to the top chamber of the Transwell, and RPMI-1640 medium supplemented with 20% FBS was added to the bottom chamber. After incubation for 24 h at 37 °C, cells across pores were fixed with 4% paraformaldehyde and stained with 1% crystal violet

solution. For each chamber, three fields were randomly chosen and cells were counted.

RNA stability assays

RNA stability was determined via Actinomycin D tests. When cells reached 80% confluence, the transcription process was suppressed by adding actinomycin D (5 μg/mL) (Sigma, USA). After the addition of actinomycin D, RNA samples were extracted at four time points (0, 2, 4, and 6 h). Cellular RNA was isolated from the harvested cells utilizing the cell RNA extraction protocol, followed by assessment with qRT-PCR.

Animal experiments

BALB/c-nu mice (5–6 weeks) were purchased from Sun Yat-sen University (SYSU) Animal Center. The mice were housed in a pathogen-free environment at the SYSU Animal Center. To establish a human ESCC xenograft model, 20 BALB/c-nu mice were randomly assigned to four groups, with each group consisting of five mice. Two groups of mice received a subcutaneous injection of either 2.0×10^6 Eca109 cells or 2.0×10^6 sh-METTL3-Eca109 cells. Tumor development was monitored daily. After one week, each mice was subjected to intratumoral injection of 10 μl PBS or Fn (1.0×10^7 CFU) once every two days, three times a week. The mice were sacrifices at the end of two weeks after the injection, and subsequently, the tumor, liver, and lungs were surgically removed. The following formula was used to determine tumor volume: $0.5\times$ (length $\times$ width^2). The number and dimensions of metastatic foci in the hepatic and pulmonary regions were recorded. The number of colonizing Fn in mouse tumor tissue was determined by qPCR according to a previous study [29].

Immunohistochemistry (IHC)

Tissue sections were incubated overnight with primary antibodies targeting METTL3 (1:50, CST) and c-Myc (1:50, Abcam) at 4 °C. After being washed with PBST, the sections were then incubated with an HRP-conjugated secondary antibody (1:5000, BOSTER) for 60 min at room temperature. The sections were developed for 10 s with 3-diaminobenzidine tetrahydrochloride and then were counterstained with 10% Mayer's hematoxylin. The analysis of IHC outcomes was conducted by two pathologists with extensive expertise in the field. The selection of visual fields (magnification of 100 $\times$) was carried out to identify the proportion of cells exhibiting positive staining relative to the overall number of tumor cells.

Compliance with Ethics requirements

Patient samples were obtained with the approval of the Ethics Committee of the Third Affiliated Hospital of Sun Yat-sen UniversityYuedong Hospital (No: II2023-006-01). The animal care and study protocols were approved by the Experimental Animal Ethics Committee of Sun Yat-sen University (No: SYSU-IACUC-2022–001286).

Statistical analysis

The findings are presented as the means ± standard deviations (SD) of three independent experiments. The statistical analysis involved the utilization of a two-tailed unpaired Student's *t* test to compare two groups. A p value of <0.05 was considered to be statistically significant. All the analyses were carried out with GraphPad 9.0 (GraphPad Software, CA, USA).

Results

Intratumoral F.nucleatuminfection was positively associated with METTL3 expression in ESCC tissues

Fn is reported to involve in the progression of a number of tumors types. First, through immunofluorescence, we verified that Fn was more highly enriched in four tumor tissues (T) (colorectal cancer, CRC, n = 3; breast cancer, BRCA, n = 3; ESCC, n = 3; hepatocellular carcinoma, HCC, n = 3) than in matched normal tissues (N) **(**Fig. 1**A).** We further confirmed the relative abundance of Fn-DNA in tumor and matched normal tissues of 22 freshly resected ESCC specimens using qPCR assay. As shown in Fig. 1**B**, Fn-DNA levels in cancer tissues were significantly higher than in matched normal tissues ($P < 0.001$).

Then, we analyzed the gene expression of direct regulators of the m6A modification, including methyltransferase-like 14 (METTL14), METTL3, fat mass and obesity-associated protein (FTO), Wilms' tumor 1-associated protein (WTAP), and alkB homolog 5 (ALKBH5), in TCGA datasets. The findings indicated that the METTL3 and WTAP mRNA expression levels were consistently elevated in ESCC tissues compared with normal tissues (Fig. 1**C and** Fig. S1**A**). Furthermore, we confirmed that Fn infection increased METTL3 mRNA expression in Eca109 and Kyse150 cells according to qRT-PCR (Fig. 1**D**). Western blot and IHC were subsequently performed to validate these findings further. The protein expressions of METTL3 in the ESCC tumor tissues were significantly higher than those in the matched normal tissues (n = 10) **(**Fig. 1**E–F).** Western blot studies demonstrated no immunological cross-reactivity between METTL3/GAPDH and Fn proteins **(**Fig. S1**B).**

Next, the Kaplan-Meier analysis results showed that the ESCC, BRCA, HCC and CRC patients with high METTL3 expression had shorter overall survival time than those with low METTL3 expression **(**Fig. 1**G and** Fig. S1**C).** Further multivariate and univariate Cox regression analyses with the TCGA cohort showed that METTL3 overexpression was an independent predictive factor for ESCC **(**Fig. 1**H).** Furthermore, we identified that expression of METTL3 was significantly increased in Fn-positive ESCC tissues compared with Fn-negative tissues ($P < 0.01$) by IHC staining **(**Fig. 1**I).** Moreover, the abundance of Fn was positively associated with METTL3 expression (R = 0.796, $P = 0.006$) **(**Fig. 1**J).**

In conclusion, Fn as an intratumoral bacterium that is observed in various tumor tissues, and its abundance was positively related to METTL3 expression, suggesting that intratumoral Fn might have affected the prognosis of individuals with ESCC by upregulating METTL3 expression.

Intracellular multiplication of F.nucleatum promotes METTL3 expression in tumor cells

Because Fn could be identified in several types of clinical tumor samples, we further determined the ability of Fn to invade different types of tumor cells utilizing an Fn and tumor cell coculture system. Tumor cells were incubated with Fn, followed by incubation with 100 μg/mL gentamycin to eliminate extracellular Fn. Fn and ESCC cell lines (Eca109 and Kyse150 cells), BRCA cell lines (231 and MCF7 cells), HCC cell lines (Huh7 and HepG2 cells), and CRC cell lines (HCT116 and SW480 cells) were cocultured at an MOI of 10 for 24, 48 and 72 h. Confocal laser scanning microscopy (CLSM) was used to observe the intracellular localization of Fn. As shown in Fig. 2**A,** Fn was labeled with red fluorescence in the cytoplasm of tumor cells. Moreover, the amount of intracellular Fn increased steadily for the first 24 to 72 h according to bacterial colony counts **(**Fig. 2**B).**

Then, we found that only live Fn increased METTL3 expression at a moderate multiplicity of infection (MOI = 10:1) in all these tumor cells (Fig. 2**C**). However, no significant variation in METTL3 expression was observed during incubation with the *Escherichia coli* control or heat-killed Fn (Fig. 2**C**). The same results were verified using a Fn strain that was isolated from an ESCC tissue sample (Fn-ESCC) (Fig. 2**D**). Consistently, IF staining showed an enhanced fluorescence intensity of METTL3 in the nucleus at 24 h post Fn infection (Fig. 2**E**). Altogether, these results indicated that Fn not only could survive and multiply inside tumor cells but also that intracellular Fn could dramatically upregulate METTL3 expression in tumor cells.

*Upregulated METTL3 facilitates the intracellular multiplication of **F. nucleatum** and promotes the malignant behavior of ESCC cells*

To further verify the function of Fn-induced METTL3 expression in both bacteria and host cells, we constructed stable METTL3-knockdown (sh-METTL3) and METTL3-overexpression (oe-METTL3) Eca109 and Kyse150 cells. Western blot was utilized to verify METTL3 expression (Fig. 3**A and** Fig. S2**A**). The upregulated protein levels of METTL3 in the Fn-treated ESCC cells were notably reduced when we knocked down METTL3 in Eca109 and Kyse150 cells (Fig. 3**A**). As predicted, METTL3 knockdown abrogated the promotion of Fn-mediated Eca109 and Kyse150 cells proliferation ability (Fig. 3**B**). Moreover, silencing of METTL3 significantly reversed the increased cell migration ability induced by Fn (Fig. 3**C–D**), highlighting the important role of METTL3 in sustaining the functions mediated by Fn. METTL3 overexpression markedly increased ESCC cells proliferation and migration (Fig. S2**B–D**). However, treatment with Fn did not significantly increase METTL3 protein expression or the proliferation and migration of oe-METTL3 ESCC cells (Fig. S2**A–D**). Then, we analyzed Fn survival and multiplication in METTL3-knockdown and METTL3-overexpressing cells. As show in Fig. 3**E,** compared with control cells, METTL3 overexpression was beneficial for Fn multiplication in host cells, while Fn multiplication was limited in sh-METTL3 Eca109 and Kyse150 cells. Taken together, we suggest that METTL3 protects intracellular bacteria and host cells during Fn infection.

Identification of METTL3 targets in F.nucleatum-infected Eca109 cells by high-throughput RNA-Seq and m6A-Seq

To examine the changes in the m6A modification of particular genes during Fn infection, we conducted differential transcriptome sequencing and differential m6A sequencing with the aim of analyzing the changes in expression and mapping m6A modifications in Fn-infected Eca109 cells and control Eca109 cells. The techniques are shown in a concise visual representation (Fig. 4**A**). Consistent with previous research findings, the distribution of determined m6A peaks exhibited the most significant degree of enrichment proximal to the stop codon, with a relatively greater proportion observed in both the mRNA intron and mRNA exon regions (Fig. 4**B**). In these cells, the consensus motif was enriched within m6A sites (Fig. 4**C**), resembling the common m6A motif described in other studies. Consistent with previous studies[30], the m6A signal showed a higher concentration in the stop codon and 3′-untranslated regions (UTRs) of mRNA (Fig. 4**D**). This study utilized meRIP-seq and RNA-seq data to examine the associations between each peak and mRNA expression, elucidating the genomic circumstances in which alterations in the m6A and RNA levels were significant. As shown in Fig. 4**E**, compared to control cells, Fn-infected Eca109 cells had 144 hypermethylated m6A peaks and higher mRNA levels (fold changes ≥ 2, $p < 0.05$).

Furthermore, the results of the m6A sequencing analysis revealed a significant elevation in m6A peaks in areas near the stop codon of MYC mRNA after Fn infection (Fig. 4**F**). It was previously suggested that METTL3 could facilitate the translation of c-Myc in gastric cancer, which inspired us to reveal whether METTL3 could regulate the expression of c-Myc [31]. The consensus motif of METTL3 was identified (GGACU) in the m6A modification targeting the 3′ UTR of c-Myc mRNA, which was adjacent to the stop codon (Fig. 4**G**). The RNA sequencing results revealed a substantial increase in Myc expression in the group infected with Fn (log2 FC |>5, $P < 0.001$) (Fig. 4**H**). Furthermore, it was determined through gene ontology (GO) enrichment analysis that m6A modifications were present in a limited number of genes that are associated with controlling vesicle fusion, spindles, and amino acid transportation in Eca109 cells that were infected with Fn (Fig. 4**I**). KEGG pathway enrichment analysis was performed (**Fig. S3**). The gene expression profiling interactive analysis (GEPIA) database derived by TCGA illustrated that Myc expression was positively correlated with METTL3 in ESCC tissues (Fig. 4**J**). These results indicate that the increase in Fn-induced Myc expression depends on the m6A methyltransferase activity of METTL3.

F.nucleatum infection promotes the malignant behavior of ESCC via the METTL3/YTHDF1/c-Myc axis

The up-regulation of c-Myc with METTL3 activation was validated by western blot, and we confirmed that METTL3 silencing reduced c-Myc protein expression, whereas METTL3 overexpression enhanced the expression (Fig. 5**A**). In the meanwhile, the protein levels of c-Myc were significantly increased, and METTL3 knockdown inhibited the increasing of c-Myc in Fn-infected Eca109 and Kyse150 cells (Fig. 5**A**).

The direct interaction between METTL3 and c-Myc mRNA was confirmed by immunoprecipitation of RNA followed by qPCR (RIP-qPCR), which confirmed that c-Myc mRNA is a target of METTL3 (Fig. 5**B**). The relative normalized luciferase activities of the wild-type and mutant c-Myc 3′UTR reporter vectors in control and METTL3-knockdown Eca109 and Kyse150 cells were compared. In addition, a significant induction in luciferase activity was observed in the wild-type 3′UTR of c-Myc in METTL3-knockdown cells relative to control cells (Fig. 5**C**). The results indicated that the modulation of c-Myc expression was controlled through METTL3-associated m6A modification.

To further confirm that m6A modifications contribute to the regulation of c-Myc expression, Eca109 and Kyse150 cells were treated with the global methylation inhibitor 3-deazaadenosine (DAA). Treatment with DAA significantly reduced the mRNA and protein expression of c-Myc (Fig. 5**D**). Actinomycin D was used to stop transcription in Eca109 and Kyse150 cells infected with Fn. The qRT-PCR analysis results suggested that Fn significantly prolonged the half-life of c-Myc mRNA in Eca109 and Kyse150 cells (Fig. 5**E**). The increased transcript stability of METTL3 targets occurs through an m6A-dependent mechanism that is mediated by YTHDF1[32]. RIP-qPCR unveiled that METTL3 inhibition could impair the direct interaction within YTHDF1 and c-Myc mRNA in Eca109 cells, indicating the close connection within METTL3, YTHDF1, and c-Myc mRNA (Fig. 5**F**). Our findings demonstrated that knockdown of YTHDF1 significantly decreased the expression of c-Myc in Eca109 cells (Fig. 5**G**). These results suggest that the methylated c-Myc mRNA was recognized by YTHDF1, and METTL3/YTHDF1 enhanced its mRNA stability.

To further determine whether Fn exerted oncogenic functions in a c-Myc dependent manner, we performed c-Myc loss of function assays in ESCC cells. The upregulated protein levels of c-Myc in Fn-treated ESCC cells were significantly decreased when we silenced c-Myc in Eca109 and Kyse150 cells (Fig. 5**H**). Cell growth was assessed via CCK-8 and colony formation assays. As expected, c-Myc knockdown abrogated the increase in proliferation of Fn-

infected Eca109 and Kyse150 cells (Fig. 5**I–J**). Cell migration was evaluated with scratch wound healing and Transwell assays.

Silencing of c-Myc significantly reversed the increased cell migration ability induced by Fn (Fig. 5**K–L**), highlighting the important role of c-Myc in sustaining the functions mediated by Fn. These findings suggested that Fn infection upregulated the METTL3/c-Myc axis to promote ESCC cells proliferation and migra-

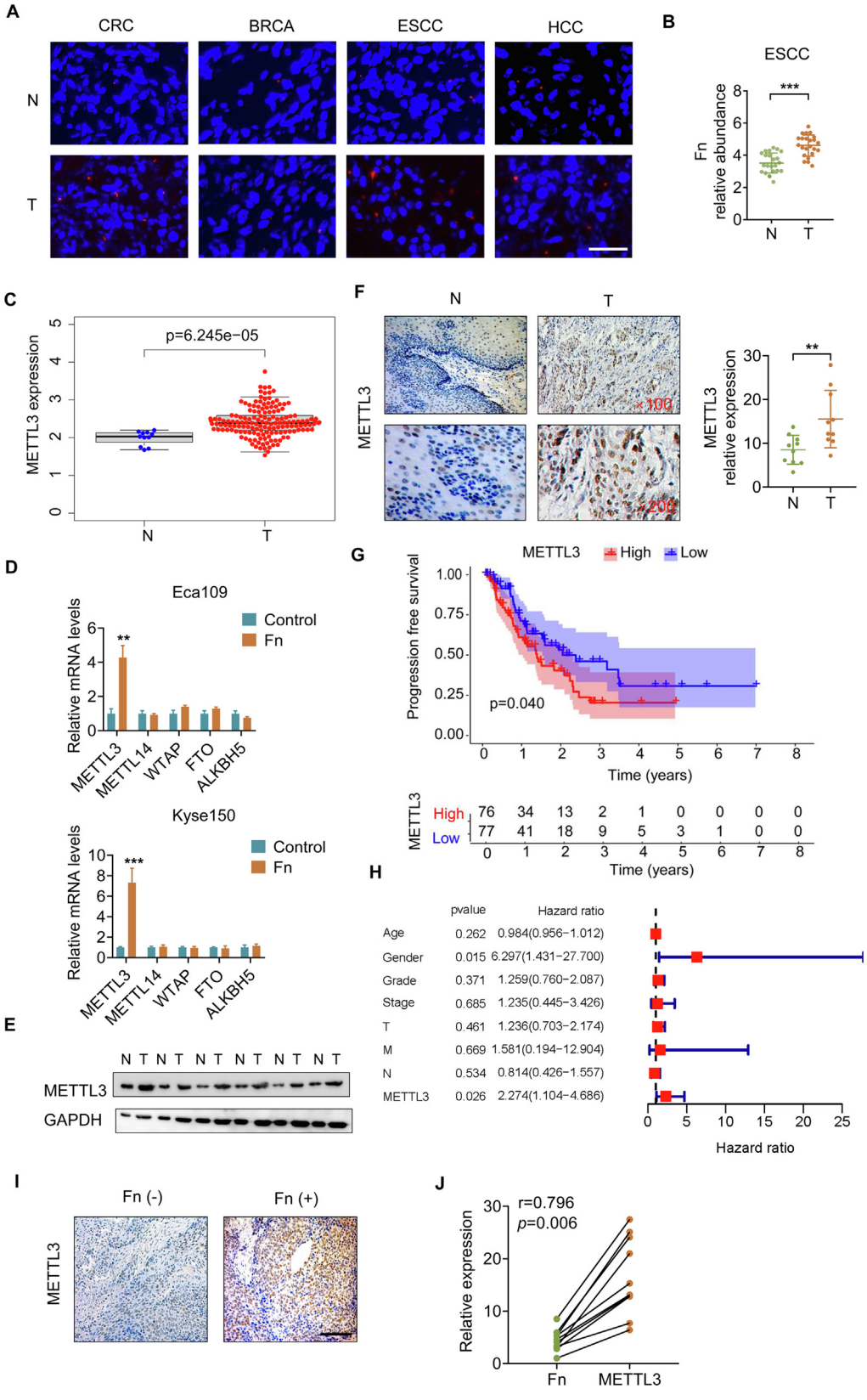

tion; these results confirmed that c-Myc was a functional target of METTL3-mediated m6A modification in ESCC.

F.nucleatum accelerates ESCC tumorigenesis and metastasis through METTL3-mediated c-Myc mRNA m6A modification in vivo

To validate the potential role of METTL3 in tumor growth *in vivo*, a human ESCC xenograft model was established in BALB/c nude mice through the subcutaneous (*s.c.*) injection of Eca109 cells, sh-METTL3 Eca109 cells, or oe-METTL3 Eca109 cells. Fig. 6**A** provides a diagram of the experiment. After 24 days, the tumors were extracted surgically (Fig. 6**B**). We observed that Fn infection increased tumor growth, while knockdown of METTL3 in Eca109 cells obviously inhibited Fn-induced tumor growth (Fig. 6**C–D**). Furthermore, data obtained from gross images and lung H&E staining analysis demonstrated a significant increase in the numbers of metastatic lesions after Fn administration. However, knockdown of METTL3 in Eca109 cells resulted in a notable inhibition of Fn-induced lung metastasis (Fig. 6**E–G**). Moreover, METTL3 and c-Myc protein levels were evaluated using IHC staining and western blot analysis (Fig. 6**H–I**). In addition, compared to the Eca109-tumor control tissues, the abundance of Fn-DNA is higher in oe-METTL3 Eca109-tumor tissues, but lower in sh-METTL3 tumor tissues by qPCR analysis (Fig. 6**J**). The results showed that Fn infection and METTL3 overexpression increased c-Myc expression, and coincidently METTL3 knockdown suppressed c-Myc expression. Collectively, these results suggest that METTL3 is a vital gene for ESCC growth and metastasis, increasing the abundance of Fn in tumor tissues. Moreover, Fn promotes ESCC aggressiveness and metastasis by upregulating the expression of c-Myc.

Discussion

In recent years, accumulating evidence reveals that METTL3 performs essential functions in m6A modification in various cancers, including functions that are both dependent and independent of its m6A RNA methyltransferase activity. Our study supported the upregulated expression of METTL3 in ESCC tissues and correlated with prognosis of ESCC patients. According to our study, most studies demonstrated that METTL3 promotes ESCC development and could potentially function as a prognostic biomarker and therapeutic target in ESCC [8,22,23,32].

Currently, there are few studies on bacteria-influenced m6A methylation in host cells. Most of bacterial infection causing destruction of host cells, it is difficult to keep the infected-host cells alive *in vitro*. Interestingly, a recent study showed that there was no significant changes in the protein and mRNA levels of the 'writers' (METTL3/14) and 'erasers' (FTO/ALKBH5) during enterotoxigenic *E. coli* K88 infection [33]. Consistently, in our study, infection with a low dose of control bacteria, *E. coli* DH5a, which has limited cytotoxicity in host cells, also did not alter the expression of METTL3 in ESCC cells. Very differently, as the most crucial member of the microbiota of CRC and ESCC tissues, Fn promotes proliferation but does not kill tumor cells [10,34]. We observed that METTL3 is upregulated in cells treated with live Fn, which can invade and proliferate inside host cells, but dead Fn cannot affect host METTL3 expression, suggesting that only intracellular pathogens might influence host RNA methylation. These results suggested that Fn, as an intracellular bacterium, develops a strategy to survive inside cells by hijacking tumor host cells.

Similarly, as intracellular pathogens, viral infection could influence the host cellular m6A epitranscriptome [35], although the specific functions and mechanisms of m6A in infected host cells are not well known. Some oncoviruses directly contribute to the transformation and proliferation of host cells by regulating METTL3. For example, high expression of METTL3 was observed in HPV-positive head and neck squamous cell carcinoma tissues [36], and METTL3 was found to be upregulated in gastric cancer cells overexpressing ebv-circRPMS1 [37]. Moreover, HBV-HBx proteins were reported to recruit METTL3 to affect m6A modification in host cells [38]. In contrast, acute viral infection which result in host cell death decreased the expression of METTL3. For example, METTL3 expression is reduced and inflammatory genes are induced in patients with severe coronavirus disease 2019 (COVID-19) [39]. These results further support that carcinogenic microbes influence the m6A of host cells by increasing but not decreasing the expression of METTL3.

We note a contrary conclusion with our study. A recent study reported mentioned that Fn decreases m6A levels and METTL3 expression in CRC[26]. As we mentioned above, Fn infection increased METTL3 expression in ESCC cells and ESCC xenograft mice. We also confirmed the elevated expression level of METTL3 in CRC, HCC, and BRCA cells that were infected with Fn. The same results were also verified using a Fn strain that was isolated from an ESCC tissue sample. Indeed, data from the TCGA databases showed METTL3 overexpression in CRC metastatic tissues, and METTL3 overexpression was related to a poor prognosis [10,40]. Furthermore, Overexpression of METTL3 was shown to promote tumor growth and metastasis of CRC, and silencing of METTL3 suppressed CRC in mice [40,41]. Therefore, we are sure that Fn infection can increase but not decrease the expression of METTL3 in various tumor cells.

Interestingly, METTL3 is frequently up-regulated and contributes to tumor progression in several malignancies which may be attributed to infections. The upregulation of METTL3 was observed in liver and nasopharyngeal carcinoma cancer [42,43], and was discovered to be an independent predictive factor of recurrence-free survival[44]. Notably, the level of m6A RNA modification was significantly increased in gastric cancer, and METTL3 was the critical modulator of m6A RNA modification. Furthermore,

Fig. 1. *F. nucleatum* was enriched in various tumor tissues and was positively related to METTL3 expression in ESCC. **(A)** Representative images of human breast cancer (BRCA), esophageal squamous cell carcinoma (ESCC), and hepatocellular carcinoma (HCC) tumor tissues and matched normal tissues using immunofluorescence staining of Fn. N: normal tissues; T: tumor tissues. Red color (Fn), Blue color (nucleus). Scale bar: 20 μm. **(B)** Fn abundance in 22 ESCC tumor tissues and matched normal tissues was measured using qPCR. N: normal tissues; T: tumor tissues. Data are presented as mean ± SD. The significant difference among the groups, $^{***}P < 0.001$. **(C)** Expression of METTL3 in tumor tissues and normal tissue in the TCGA ESCC cohort. N: normal tissues; T: tumor tissues. **(D)** Fn infected (MOI = 10:1) Eca109 and Kyse150 cells for 24 h. mRNA expression was measured using qRT-PCR. Data are presented as mean ± SD. The significant difference among the groups, $^{**}P < 0.01$, $^{***}P < 0.001$. **(E)** Western blot analysis of METTL3 expression in 6 ESCC tumor tissues and matched normal tissues. N: normal tissues; T: tumor tissues. **(F)** Representative images of immunohistochemical staining of human ESCC tumor tissues and matched normal tissues (n = 10) using an anti-Fn antibody. N: normal tissues; T: tumor tissues. Left images magnification × 100/ ×200; right, statistical results of the quantification of the gray values from immunohistochemistry. Data are presented as mean ± SD. The significant difference among the groups, $^{**}P < 0.01$. **(G)** Progression-free survival (PFS) analysis and **(H)** Cox regression analysis (univariate and multivariate) of METTL3 in the TCGA ESCC cohort. **(I)** Representative images of immunohistochemical staining of Fn-positive (Fn +) and Fn-negative (Fn-) ESCC tumor tissues using an anti-METTL3 antibody. Scale bar: 10 μm. **(J)** Correlation analysis of Fn abundance and METTL3 expression in 10 ESCC tumor tissues. (For interpretation of the references to color in this figure legend, the reader is referred to the web version of this article.)

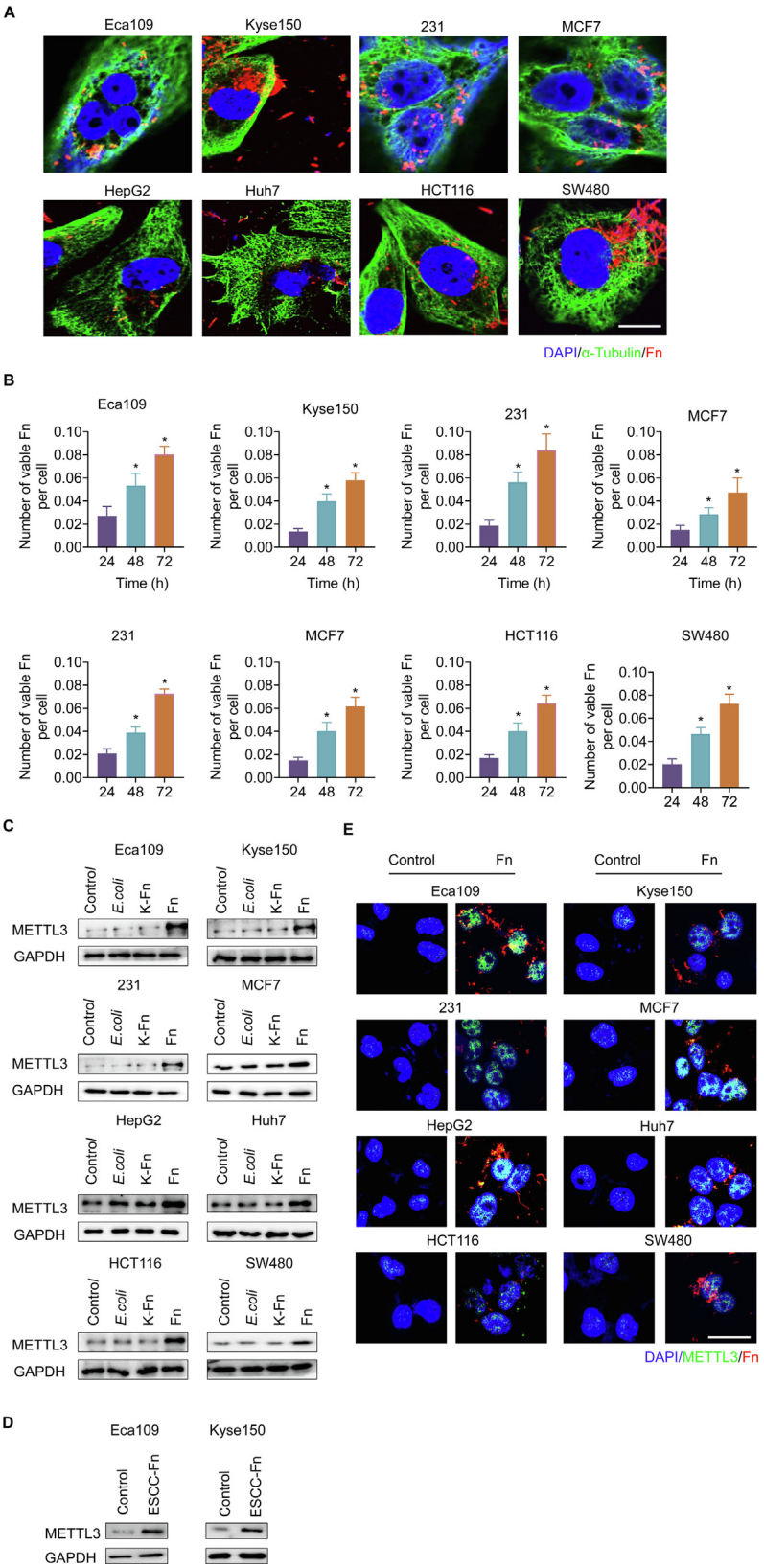

Fig. 2. *F. nucleatum* can survive, proliferate and upregulate the expression of METTL3 in ESCC, BRCA, HCC, and CRC cell lines. **(A)** Immunofluorescence visualization of α-tubulin and Fn in ESCC cells, BRCA cells, HCC cells, and CRC cells. Cells were infected with Fn (MOI = 10:1) for 48 h. Scale bar: 100 μm. **(B)** Intracellular bacterial proliferation was assessed by gentamycin protection assay. The numbers of viable bacteria per cell were determined by the serial dilution method. Data are presented as mean ± SD. The significant difference among the groups, $^{*}P < 0.05$. **(C)** Western blot analysis of METTL3 expression in ESCC, BRCA, HCC, and CRC cells after infection with *E. coli* (MOI = 1:100), Fn (MOI = 10:1), or K-Fn (MOI = 10:1) for 48 h. **(D)** Western blot analysis of METTL3 expression in ESCC cells after infection with ESCC-Fn (Fn isolated from ESCC tissue sample; MOI = 10:1) for 48 h. **(E)** Representative images of ESCC, BRCA, HCC, and CRC cells after infection with Fn (MOI = 10:1) for 48 h using immunofluorescence (IF) staining of Fn. Red color (Fn), Blue color (nucleus). Immunofluorescence analysis of METTL3 in ESCC, BRCA, HCC, and CRC cells after infection with Fn (MOI = 10:1) for 48 h. Scale bar: 50 μm. (For interpretation of the references to color in this figure legend, the reader is referred to the web version of this article.)

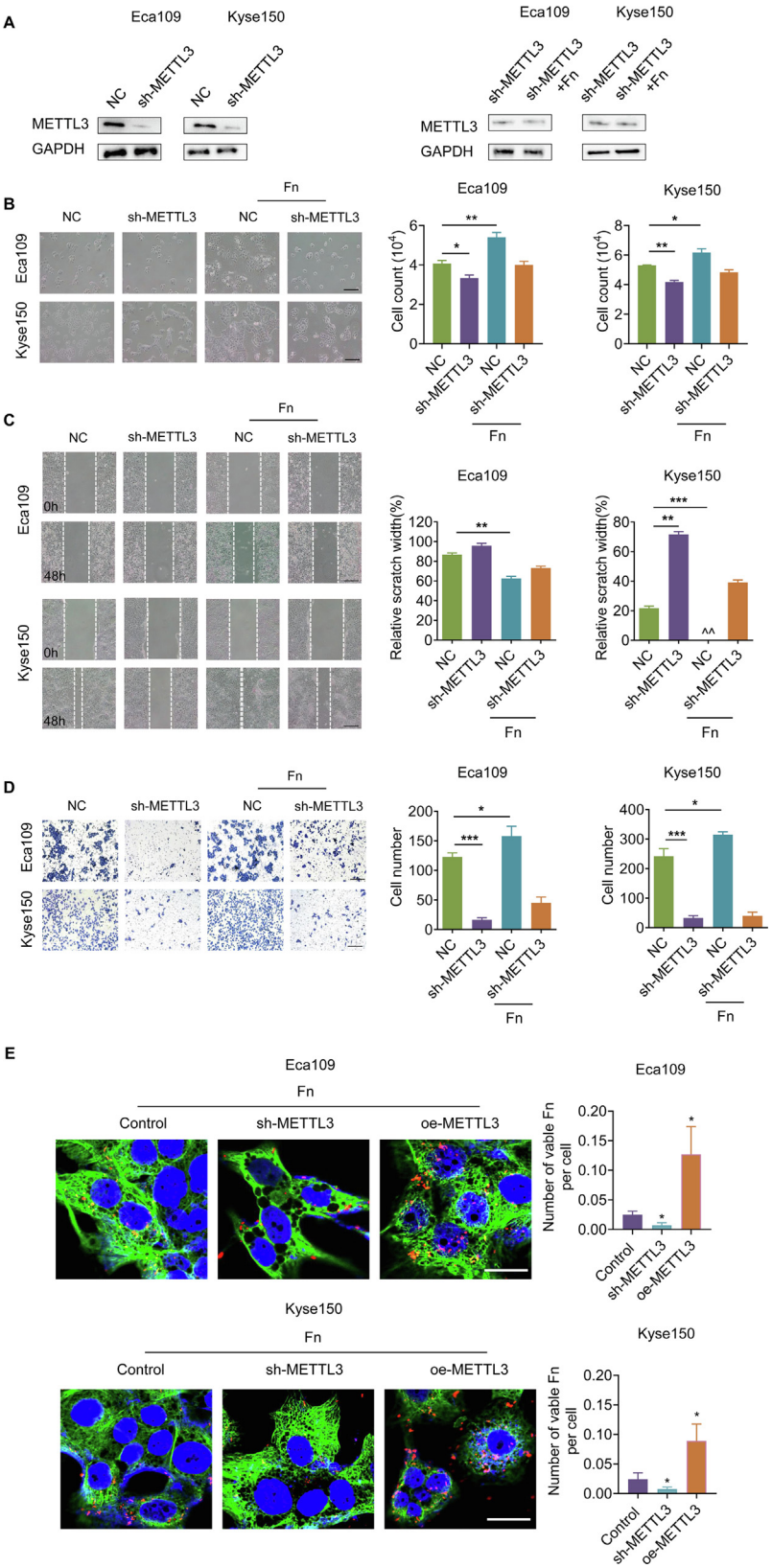

Fig. 3. METTL3 is involved in *F. nucleatum*-induced ESCC cells proliferation and migration *in vitro*. ESCC cells treated with PBS (NC), ESCC cells stably infected with lentivirus-based METTL3 shRNA (sh-METTL3), or sh-METTL3 ESCC cells infected with Fn (MOI = 10:1). **(A)** Western blot analysis of METTL3 was performed. **(B)** Cell proliferation analysis assays were performed. Scale bar: 200 μm Statistical results are presented in the right panels. Data are presented as the mean ± SD. The significant difference among the groups, $^{*}P < 0.05$, $^{**}P < 0.01$. **(C)** Scratch wound assays were performed. Scale bar: 200 μm. Statistical results are presented in the right panels. Data are presented as the mean ± SD. The significant difference among the groups, $^{**}P < 0.01$, $^{***}P < 0.001$. **(D)** Transwell assays were performed. Scale bar: 200 μm. Statistical results are presented in the right panels. Data are presented as the mean ± SD. The significant difference among the groups, $^{*}P < 0.05$, $^{***}P < 0.001$. Intracellular Fn assays were performed. Scale bar: 30 μm, statistical results are presented in the right panels. Data are presented as mean ± SD. The significant difference among the groups, $^{*}P < 0.05$.

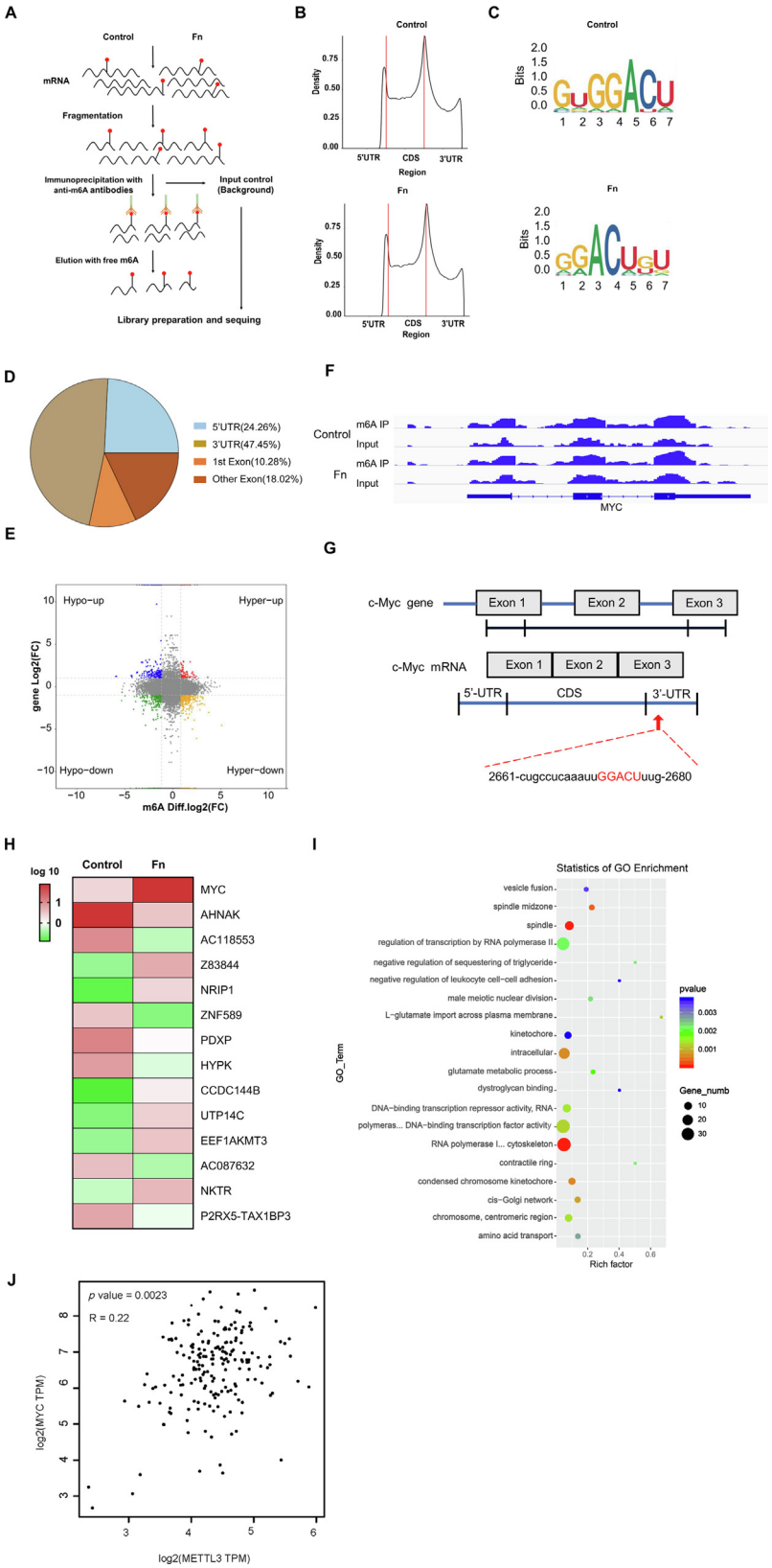

Fig. 4. METTL3-mediated increase in m6A modification of MYC mRNA in ESCC cells infected with *F. nucleatum*. **(A)** m6A MeRIP sequencing flow chart. **(B)** Metagene profiles of the distribution of m6A across the transcriptome and **(C)** consensus sequence motif for m6A methylation in Eca109 cells that were uninfected or infected with Fn (MOI = 10:1) for 48 h. **(D)** The proportions of m6A peak distribution in the 5′UTR, CDS, stop codon, or 3′UTR across the entire set of mRNA transcripts. **(E)** Distribution of peaks (fold change > 1.0, $P < 0.05$) with an obvious change in both the RNA expression level and m6A level in Fn-infected Eca109 cells relative to Eca109 cells. **(F)** Representative m6A modification of Myc by m6A in Eca109 cells. **(G)** The location of the m6A site in c-Myc mRNA. **(H)** Heatmap showing the differential gene expression patterns between Fn-infected and uninfected Eca109 cells (fold change > 2, $P < 0.01$). **(I)** Gene ontology and enrichment analysis of m6A-modified genes. **(J)** The expression of METTL3 showed a positive relationship with that of Myc in the public database (GEPIA).

METTL3 expression was substantially elevated in gastric cancer tissues and was related to a poor prognosis [45]. Furthermore, METTL3 overexpression has been observed to exacerbate LPS-induced cellular inflammation [46]. Additionally, we further verified that Fn upregulated the expression of METTL3 in ESCC. Multiple studies from other groups also indicated that intratumoral Fn confers chemoresistance and predicts a high risk of metastasis in ESCC [25]. Together with these results, we suggest that intratumoral Fn might exacerbate inflammation by upregulating the expression of METTL3 to promote tumor progression.

Notably, METTL3 was frequently upregulated in human CRC tissues and promoted CRC progression though enhancing MYC expression [47]. Similar results were observed in bladder cancer [48,49], gastric cancer [31,50], and prostate carcinoma [51]. These studies indicated that METTL3 improved the expression of c-Myc (MYC) by elevating the m6A levels of the c-Myc mRNA transcript, playing oncogenic roles in these tumors. Consistent with these results, we further showed that Fn functions as an oncogenic bacterium to enhance the METTL3/c-Myc axis by increasing m6A modification.

Conclusion

Overall, our results indicated that Fn invades tumor cells to promote METTL3 expression, which is beneficial for the survival and proliferation of both the intracellular bacteria and host cells. Furthermore, METTL3 is highly expressed in Fn-positive ESCC tumor tissues. The clinical relevance and significance of our findings are evidenced by the correlation of upregulated METTL3 expression in human ESCC tissues and poor prognosis in ESCC patients. Intratumoral Fn mediated the upregulation of METTL3 considerably augmented its oncogenic function via increasing m6A levels of MYC in ESCC. Our work reveals the oncogenic roles of Fn and suggests a critical mechanism of ESCC progression.

Declaration of Competing Interest

The authors declare that they have no known competing financial interests or personal relationships that could have appeared to influence the work reported in this paper.

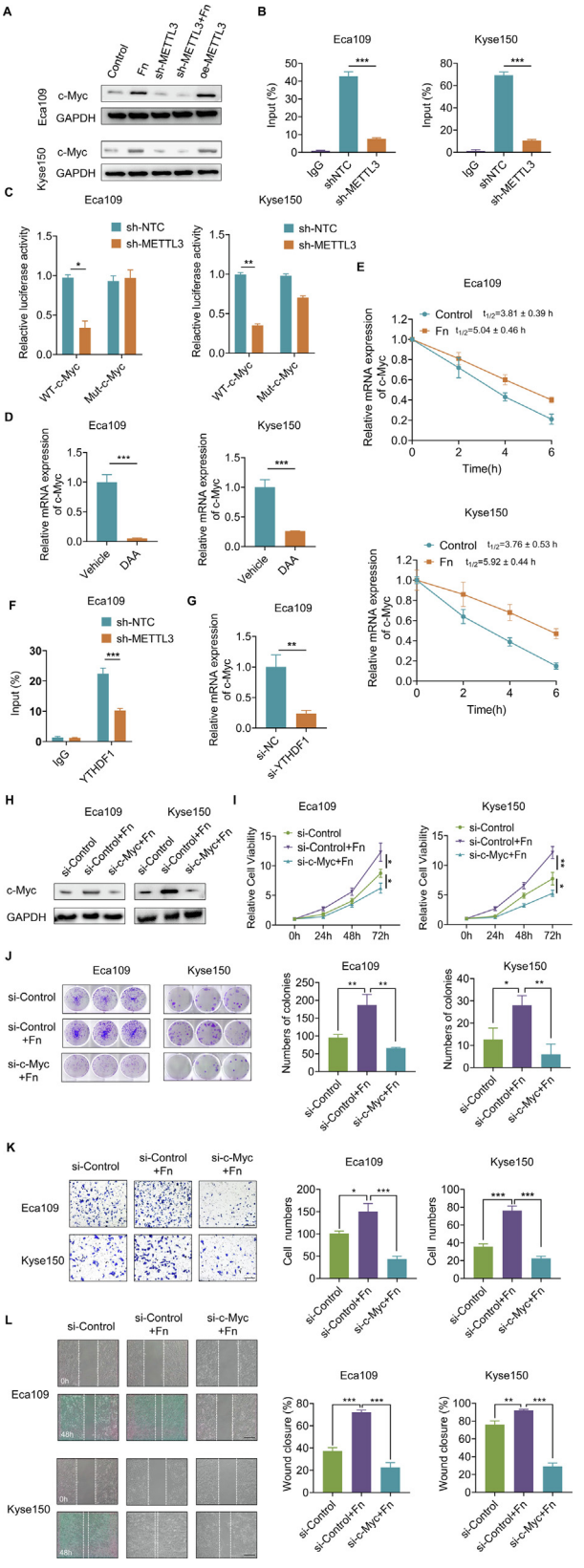

Fig. 5. C-myc was a downstream target ofMETTL3-mediated m6A modification, and subsequent binding of YTHDF1 enhanced c-Myc expression. (A) Western blot analysis of c-Myc expression in ESCC cells. **(B)** RNA immunoprecipitation following qPCR (RIP-qPCR) showed the interaction within METTL3 protein and c-Myc mRNA. Data are presented as mean ± SD. The significant difference among the groups, $^{***}P < 0.001$. **(C)** Luciferase vectors with the WT-c-Myc gene or the c-Myc gene with mutated m6A nucleotides were transfected into ESCC cells with or without METTL3 knockdown. The relative luciferase activity was measured. Data are presented as mean ± SD. The significant difference among the groups, $^{*}P < 0.05$, $^{**}P < 0.01$. **(D)** qRT-PCR analysis of c-Myc expression in ESCC cells treated with 10 μM 3-deazaadenosine (DAA) for 48 h. DAA is a methylation inhibitor. Data are presented as mean ± SD. The significant difference among the groups, $^{***}P < 0.001$. **(E)** ESCC cells were pretreated with Fn or PBS for 2 h. The remaining c-Myc mRNA levels were measured using qRT-PCR at the indicated time points after actinomycin D (Act-D; 5 μg/mL) treatment. **(F)** RIP-qPCR unveiled the interaction within YTHDF1 and c-Myc mRNA after METTL3 inhibition. Data are presented as mean ± SD. The significant difference among the groups, $^{**}P < 0.01$, $^{***}P < 0.001$.**(G)** Eca109 cells were transfected with or without a YTHDF1-siRNA. The relative mRNA expression levels of c-Myc were measured using qRT-PCR. Data are presented as mean ± SD. The significant difference among the groups, $^{**}P < 0.01$. ESCC cells transfected with the indicated siRNAs were cocultured with Fn or PBS control. **(H)** Western blot analysis of c-Myc was performed. **(I)** CCK8 assays were performed. Data are presented as the mean ± SD. The significant difference among the groups, $^{*}P < 0.05$, $^{**}P < 0.01$. **(J)** Colony formation assays were performed. Statistical results are presented in the right panels. Data are presented as the mean ± SD. The significant difference among the groups, $^{*}P < 0.05$, $^{**}P < 0.01$. **(K)** Transwell assays were performed. Scale bar: 200 μm. Statistical results are presented in the right panels. Data are presented as the mean ± SD. The significant difference among the groups, $^{*}P < 0.05$, $^{***}P < 0.001$. **(L)** Scratch wound assays were performed. Scale bar:200 μm. Statistical results are presented in the right panels. Data are presented as the mean ± SD. The significant difference among the groups, $^{**}P < 0.01$, $^{***}P < 0.001$.

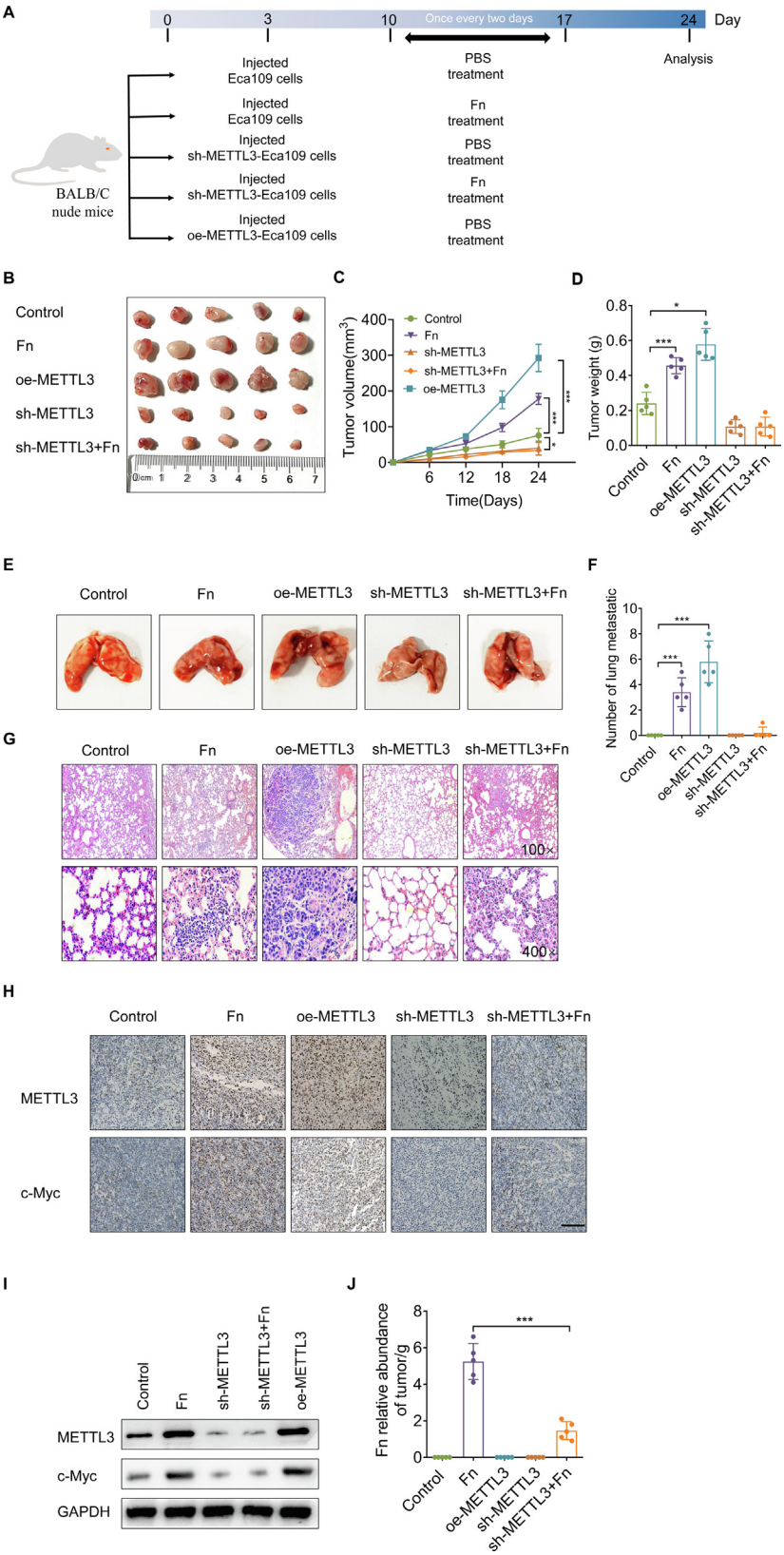

Fig. 6. Fn promotes ESCC proliferation and metastasis by upregulating METTL3. **(A)** A flow chart showing the *in vivo* experimental design. METTL3-knockdown (sh-METTL3) or METTL3-overexpressing(oe-METTL3) Eca109 cells were subcutaneously injected into nude mice (n = 5). **(B)** Representative images showing xenografts in nude mice. 24 days later, **(C)** tumor volumes and **(D)** weights were measured. Data are presented as the mean ± SD. The significant difference among the groups, $^{*}P < 0.05$, $^{***}P < 0.001$. **(E)** Representative images of the lung metastatic nodules and **(F)** quantitative analysis. Data are presented as the mean ± SD. The significant difference among the groups, $^{***}P < 0.001$. **(G)** Histopathological examination of the lung tissue sections. Magnification × 100/×400. **(H)** Immunohistochemical staining and **(I)** western blot analysis of METTL3 and c-Myc expression in tumor tissues. Scale bar, 200 μm. **(J)** Fn abundance in tumor tissue samples was measured using qPCR. Data are presented as the mean ± SD. The significant difference among the groups, $^{***}P < 0.001$.

Data availability

The raw m6A-RIP and m6A sequencing data files are available at the Gene Expression Omnibus database (GEO), identifier GSE240349. The remaining data are shown in the manuscript and its Supporting Information files.

Acknowledgments

This work was financially supported by the National Natural Science Foundation of China (No. 82172890) and the Special Financial grant from the China Postdoctoral Science Foundation (No. 2022TQ0384).

Appendix A. Supplementary data

Supplementary data to this article can be found online at https://doi.org/10.1016/j.jare.2023.08.014.

References

[1] Huang W, Chen TQ, Fang K, Zeng ZC, Ye H, Chen YQ. N6-methyladenosine methyltransferases: functions, regulation, and clinical potential. J Hematol Oncol 2021;14:117. doi: https://doi.org/10.1186/s13045-021-01129-8.
[2] Zaccara S, Ries RJ, Jaffrey SR. Reading, writing and erasing mRNA methylation. Nat Rev Mol Cell Biol 2019;20:608–24. doi: https://doi.org/10.1038/s41580-019-0168-5.
[3] Jiang X, Liu B, Nie Z, Duan L, Xiong Q, Jin Z, et al. The role of m6A modification in the biological functions and diseases. Signal Transduct Target Ther 2021;6:74. doi: https://doi.org/10.1038/s41392-020-00450-x.
[4] Zeng C, Huang W, Li Y, Weng H. Roles of METTL3 in cancer: mechanisms and therapeutic targeting. J Hematol Oncol 2020;13:117. doi: https://doi.org/10.1186/s13045-020-00951-w.
[5] Shulman Z, Stern-Ginossar N. The RNA modification N(6)-methyladenosine as a novel regulator of the immune system. Nat Immunol 2020;21:501–12. doi: https://doi.org/10.1038/s41590-020-0650-4.
[6] Xu P, Ge R. Roles and drug development of METTL3 (methyltransferase-like 3) in anti-tumor therapy. Eur J Med Chem 2022;230:. doi: https://doi.org/10.1016/j.ejmech.2022.114118114118.
[7] Chen H, Gao S, Liu W, Wong CC, Wu J, Wu J, et al. RNA N(6)-Methyladenosine Methyltransferase METTL3 Facilitates Colorectal Cancer by Activating the m(6)A-GLUT1-mTORC1 Axis and Is a Therapeutic Target. Gastroenterology 2021;160:1284–300 e16. doi: https://doi.org/10.1053/j.gastro.2020.11.013.
[8] Wang W, Shao F, Yang X, Wang J, Zhu R, Yang Y, et al. METTL3 promotes tumour development by decreasing APC expression mediated by APC mRNA N(6)-methyladenosine-dependent YTHDF binding. Nat Commun 2021;12:3803. doi: https://doi.org/10.1038/s41467-021-23501-5.
[9] Xia TL, Yan SM, Yuan L, Zeng MS. Upregulation of METTL3 Expression Predicts Poor Prognosis in Patients with Esophageal Squamous Cell Carcinoma. Cancer Manag Res 2020;12:5729–37. doi: https://doi.org/10.2147/CMAR.S245019.
[10] Li T, Hu PS, Zuo Z, Lin JF, Li X, Wu QN, et al. METTL3 facilitates tumor progression via an m(6)A-IGF2BP2-dependent mechanism in colorectal carcinoma. Mol Cancer 2019;18:112. doi: https://doi.org/10.1186/s12943-019-1038-7.
[11] Nejman D, Livyatan I, Fuks G, Gavert N, Zwang Y, Geller LT, et al. The human tumor microbiome is composed of tumor type-specific intracellular bacteria. Science 2020;368:973–80. doi: https://doi.org/10.1126/science.aay9189.
[12] Fu A, Yao B, Dong T, Chen Y, Yao J, Liu Y, et al. Tumor-resident intracellular microbiota promotes metastatic colonization in breast cancer. Cell 2022;185:1356–72 e26. doi: https://doi.org/10.1016/j.cell.2022.02.027.
[13] Xue Y, Xiao H, Guo S, Xu B, Liao Y, Wu Y, et al. Indoleamine 2,3-dioxygenase expression regulates the survival and proliferation of Fusobacterium nucleatum in THP-1-derived macrophages. Cell Death Dis 2018;9:355. doi: https://doi.org/10.1038/s41419-018-0389-0.
[14] Parhi L, Alon-Maimon T, Sol A, Nejman D, Shhadeh A, Fainsod-Levi T, et al. Breast cancer colonization by Fusobacterium nucleatum accelerates tumor growth and metastatic progression. Nat Commun 2020;11:3259. doi: https://doi.org/10.1038/s41467-020-16967-2.
[15] Yamamura K, Baba Y, Nakagawa S, Mima K, Miyake K, Nakamura K, et al. Human Microbiome Fusobacterium Nucleatum in Esophageal Cancer Tissue Is Associated with Prognosis. Clin Cancer Res 2016;22:5574–81. doi: https://doi.org/10.1158/1078-0432.CCR-16-1786.
[16] Chen WD, Zhang X, Zhang MJ, Zhang YP, Shang ZQ, Xin YW, et al. Salivary Fusobacterium nucleatum serves as a potential diagnostic biomarker for gastric cancer. World J Gastroenterol 2022;28:4120–32. doi: https://doi.org/10.3748/wjg.v28.i30.4120.
[17] Udayasuryan B, Ahmad RN, Nguyen TTD, Umana A, Monet Roberts L, Sobol P, et al. Fusobacterium nucleatum induces proliferation and migration in pancreatic cancer cells through host autocrine and paracrine signaling. Sci Signal 2022;15:eabn4948. doi: https://doi.org/10.1126/scisignal.abn4948.
[18] Wang N, Fang JY. Fusobacterium nucleatum, a key pathogenic factor and microbial biomarker for colorectal cancer. Trends Microbiol 2022. doi: https://doi.org/10.1016/j.tim.2022.08.010.
[19] Galeano Nino JL, Wu H, LaCourse KD, Kempchinsky AG, Baryiames A, Barber B, et al. Effect of the intratumoral microbiota on spatial and cellular heterogeneity in cancer. Nature 2022;611:810–7. doi: https://doi.org/10.1038/s41586-022-05435-0.
[20] Sung H, Ferlay J, Siegel RL, Laversanne M, Soerjomataram I, Jemal A, et al. Global Cancer Statistics 2020: GLOBOCAN Estimates of Incidence and Mortality Worldwide for 36 Cancers in 185 Countries. CA Cancer J Clin 2021;71:209–49. doi: https://doi.org/10.3322/caac.21660.
[21] Li J, Li Z, Xu Y, Huang C, Shan B. METTL3 Facilitates Tumor Progression by COL12A1/MAPK Signaling Pathway in Esophageal Squamous Cell Carcinoma. J Cancer 2022;13:1972–84. doi: https://doi.org/10.7150/jca.66830.
[22] Zhou Y, Guo S, Li Y, Chen F, Wu Y, Xiao Y, et al. METTL3 Is Associated With the Malignancy of Esophageal Squamous Cell Carcinoma and Serves as a Potential Immunotherapy Biomarker. Front Oncol 2022;12:. doi: https://doi.org/10.3389/fonc.2022.824190824190.
[23] Zou J, Zhong X, Zhou X, Xie Q, Zhao Z, Guo X, et al. The M6A methyltransferase METTL3 regulates proliferation in esophageal squamous cell carcinoma. Biochem Biophys Res Commun 2021;580:48–55. doi: https://doi.org/10.1016/j.bbrc.2021.05.048.
[24] Nomoto D, Baba Y, Liu Y, Tsutsuki H, Okadome K, Harada K, et al. Fusobacterium nucleatum promotes esophageal squamous cell carcinoma progression via the NOD1/RIPK2/NF-kappaB pathway. Cancer Lett 2022;530:59–67. doi: https://doi.org/10.1016/j.canlet.2022.01.014.
[25] Li Z, Shi C, Zheng J, Guo Y, Fan T, Zhao H, et al. Fusobacterium nucleatum predicts a high risk of metastasis for esophageal squamous cell carcinoma. BMC Microbiol 2021;21:301. doi: https://doi.org/10.1186/s12866-021-02352-6.
[26] Chen S, Zhang L, Li M, Zhang Y, Sun M, Wang L, et al. Fusobacterium nucleatum reduces METTL3-mediated m(6)A modification and contributes to colorectal cancer metastasis. Nat Commun 2022;13:1248. doi: https://doi.org/10.1038/s41467-022-28913-5.
[27] Xu Q, Lu X, Li J, Feng Y, Tang J, Zhang T, et al. Fusobacterium nucleatum induces excess methyltransferase-like 3-mediated microRNA-4717-3p maturation to promote colorectal cancer cell proliferation. Cancer Sci 2022;113:3787–800. doi: https://doi.org/10.1111/cas.15536.
[28] Gong C, Maquat LE. lncRNAs transactivate STAU1-mediated mRNA decay by duplexing with 3' UTRs via Alu elements. Nature 2011;470:284–8. doi: https://doi.org/10.1038/nature09701.
[29] Guo S, Li L, Xu B, Li M, Zeng Q, Xiao H, et al. A Simple and Novel Fecal Biomarker for Colorectal Cancer: Ratio of Fusobacterium Nucleatum to Probiotics Populations, Based on Their Antagonistic Effect. Clin Chem 2018;64:1327–37. doi: https://doi.org/10.1373/clinchem.2018.289728.
[30] Zhang L, Zhang Y, Liu J, Li H, Liu B, Zhao T. N6-methyladenosine mRNA methylation is important for the light response in soybean. Front Plant Sci 2023;14:1153840. doi: https://doi.org/10.3389/fpls.2023.1153840.
[31] Yang DD, Chen ZH, Yu K, Lu JH, Wu QN, Wang Y, et al. METTL3 Promotes the Progression of Gastric Cancer via Targeting the MYC Pathway. Front Oncol 2020;10:115. doi: https://doi.org/10.3389/fonc.2020.00115.
[32] Zhao W, Cui Y, Liu L, Ma X, Qi X, Wang Y, et al. METTL3 Facilitates Oral Squamous Cell Carcinoma Tumorigenesis by Enhancing c-Myc Stability via YTHDF1-Mediated m(6)A Modification. Mol Ther Nucleic Acids 2020;20:1–12. doi: https://doi.org/10.1016/j.omtn.2020.01.033.
[33] Zong X, Wang H, Xiao X, Zhang Y, Hu Y, Wang F, et al. Enterotoxigenic Escherichia coli infection promotes enteric defensin expression via FOXO6-METTL3-m(6)A-GPR161 signalling axis. RNA Biol 2021;18:576–86. doi: https://doi.org/10.1080/15476286.2020.1820193.
[34] Peng W, Li J, Chen R, Gu Q, Yang P, Qian W, et al. Upregulated METTL3 promotes metastasis of colorectal Cancer via miR-1246/SPRED2/MAPK signaling pathway. J Exp Clin Cancer Res 2019;38:393. doi: https://doi.org/10.1186/s13046-019-1408-4.
[35] Barranco C. Viral infection linked to m(6)A alterations in host mRNAs. Nat Rev Mol Cell Biol 2020;21:64–5. doi: https://doi.org/10.1038/s41580-019-0202-7.
[36] Yu R, Wei Y, He C, Zhou P, Yang H, Deng C, et al. Integrative Analyses of m6A Regulators Identify that METTL3 is Associated with HPV Status and Immunosuppressive Microenvironment in HPV-related Cancers. Int J Biol Sci 2022;18:3874–87. doi: https://doi.org/10.7150/ijbs.70674.
[37] Zhang JY, Du Y, Gong LP, Shao YT, Pan LJ, Feng ZY, et al. ebv-circRPMS1 promotes the progression of EBV-associated gastric carcinoma via Sam68-dependent activation of METTL3. Cancer Lett 2022;535:. doi: https://doi.org/10.1016/j.canlet.2022.215646215646.
[38] Kim GW, Siddiqui A. Hepatitis B virus X protein recruits methyltransferases to affect cotranscriptional N6-methyladenosine modification of viral/host RNAs. PNAS 2021;118. doi: https://doi.org/10.1073/pnas.2019455118.
[39] Li N, Hui H, Bray B, Gonzalez GM, Zeller M, Anderson KG, et al. METTL3 regulates viral m6A RNA modification and host cell innate immune responses during SARS-CoV-2 infection. Cell Rep 2021;35:. doi: https://doi.org/10.1016/j.celrep.2021.109091109091.
[40] Chen H, Pan Y, Zhou Q, Liang C, Wong CC, Zhou Y, et al. METTL3 Inhibits Antitumor Immunity by Targeting m(6)A-BHLHE41-CXCL1/CXCR2 Axis to Promote Colorectal Cancer. Gastroenterology 2022;163:891–907. doi: https://doi.org/10.1053/j.gastro.2022.06.024.

[41] Zhou D, Tang W, Xu Y, Xu Y, Xu B, Fu S, et al. METTL3/YTHDF2 m6A axis accelerates colorectal carcinogenesis through epigenetically suppressing YPEL5. Mol Oncol 2021;15:2172–84. doi: https://doi.org/10.1002/1878-0261.12898.
[42] Chen M, Wei L, Law CT, Tsang FH, Shen J, Cheng CL, et al. RNA N6-methyladenosine methyltransferase-like 3 promotes liver cancer progression through YTHDF2-dependent posttranscriptional silencing of SOCS2. Hepatology 2018;67:2254–70. doi: https://doi.org/10.1002/hep.29683.
[43] Liu ZF, Yang J, Wei SP, Luo XG, Jiang QS, Chen T, et al. Upregulated METTL3 in nasopharyngeal carcinoma enhances the motility of cancer cells. Kaohsiung J Med Sci 2020;36:895–903. doi: https://doi.org/10.1002/kjm2.12266.
[44] Liu GM, Zeng HD, Zhang CY, Xu JW. Identification of METTL3 as an Adverse Prognostic Biomarker in Hepatocellular Carcinoma. Dig Dis Sci 2021;66:1110–26. doi: https://doi.org/10.1007/s10620-020-06260-z.
[45] Wang Q, Chen C, Ding Q, Zhao Y, Wang Z, Chen J, et al. METTL3-mediated m(6)A modification of HDGF mRNA promotes gastric cancer progression and has prognostic significance. Gut 2020;69:1193–205. doi: https://doi.org/10.1136/gutjnl-2019-319639.
[46] Yang L, Wu G, Wu Q, Peng L, Yuan L. METTL3 overexpression aggravates LPS-induced cellular inflammation in mouse intestinal epithelial cells and DSS-induced IBD in mice. Cell Death Discov 2022;8:62. doi: https://doi.org/10.1038/s41420-022-00849-1.
[47] Xiang S, Liang X, Yin S, Liu J, Xiang Z. N6-methyladenosine methyltransferase METTL3 promotes colorectal cancer cell proliferation through enhancing MYC expression. Am J Transl Res 2020;12:1789–806.
[48] Cheng M, Sheng L, Gao Q, Xiong Q, Zhang H, Wu M, et al. The m(6)A methyltransferase METTL3 promotes bladder cancer progression via AFF4/NF-kappaB/MYC signaling network. Oncogene 2019;38:3667–80. doi: https://doi.org/10.1038/s41388-019-0683-z.
[49] Wang A, Chen Y, Shi L, Li M, Li L, Wang S, et al. Tumor-suppressive MEG3 induces microRNA-493-5p expression to reduce arabinocytosine chemoresistance of acute myeloid leukemia cells by downregulating the METTL3/MYC axis. J Transl Med 2022;20:288. doi: https://doi.org/10.1186/s12967-022-03456-x.
[50] Yang Z, Jiang X, Li D, Jiang X. HBXIP promotes gastric cancer via METTL3-mediated MYC mRNA m6A modification. Aging (Albany NY) 2020;12:24967–82. doi: https://doi.org/10.18632/aging.103767.
[51] Yuan Y, Du Y, Wang L, Liu X. The M6A methyltransferase METTL3 promotes the development and progression of prostate carcinoma via mediating MYC methylation. J Cancer 2020;11:3588–95. doi: https://doi.org/10.7150/jca.42338.